OPTIMAL TIME AND FREQUENCY TRANSFER USING GPS SIGNALS

David W. Allan and James A. Barnes
Time and Frequency Division
National Bureau of Standards
Boulder, Colorado 80303

Introduction

The advent of the GPS Satellite constellation makes atomic clocks available to any one who has a receiver. Proper characterization of both the clocks and the user links is essential for optimal extraction of time and frequency (T&F) information. In this paper we will consider both optimum T&F extraction from a set of GPS data, and also some near optimum and simple data processing techniques.

We consider three simple cases: case A is what we call the "common-view" approach; case B is the direct viewing of a single satellite for sample times ranging from a few seconds to a few hours; and case C is viewing a single satellite for a few minutes each day for several successive days. The common-view approach has been studied elsewhere (1-3), and the results will be reviewed as they relate to the common-mode cancellation of errors which occur when two user sites view the same satellite for the same several minutes each day, and then subtract their results to get the time difference between the two receiving sites. If one of the two receiving sites is a primary T&F reference standard, then state-of-the-art calibrations are possible. Case B allows one to use the GPS signals as a short-term T&F reference to UTC(NBS) or UTC (USNO)--thus allowing one to calibrate against a primary reference standard.

After characterizing the real data for the above three cases, we develop models from which we can design a Kalman filter. We then test this filter on simulated data, and on some real data. As we proceed it is useful to review some definitions of terms so that the language is clear. Accuracy is defined as the degree to which one can relate a measurement to some absolute reference. Stability, on the other hand, is defined as a measure of constancy--typically over selected sampling periods. We consider both the accuracy and the stability of time and frequency as well as the Fourier frequency (f) components of the instabilities of the GPS links and clocks involved. These instabilities or noise fluctuations are characterized in the time-domain by $\sigma_y(\tau)$ and "modified" $\sigma_y(\tau)$ diagrams (4,5). These noise fluctuations appear to be well characterized by power-law spectral densities(4). The "Modified Allan variance" is associated with a measurement bandwidth proportional to the reciprocal of the sample time for which the data is taken. This sample time (denoted τ_h) results in a high-frequency cut-off for the data.

We use typical performance for the models except in those instances where there is a wide range of performance. In which case we use both the worst and best case situations. We do not deal in any detail with error detection and data rejection for this could be the text of a paper all by itself. Rather we have chosen reasonable rejection and interpolation criteria in order to minimize deliterious effects on a proper characterization. The resulting filters are, therefore, appropriate for well behaved data. However, intrinsic to their optimum or near optimum nature is the ability to do error detection and data rejection.

GPS LINK AND CLOCK CHARACTERIZATION

A. Case A: GPS in common-view of two receiving sites.

The results of a previous study are reviewed in Figure 1 showing the GPS measurement limit using this common-view approach averaged across four satellites and over the approximately 3000 km baseline between NBS-Boulder and USNO. The $\tau^{-3/2}$ performance of MOD $\sigma_y(\tau)$ indicates white noise phase modulation(PM). The level of the noise is such that MOD $\sigma_y(\tau=1\text{ day})=1\text{x}10^{-13}$ for $\tau_h=600\text{s}$. The resulting RMS time fluctuations are about 5ns. Figure 1 compares these results with a "Range of performance of state-of-the-art standards", with the NBS + USNO instabilities, and with the historical Loran-C comparison method.

The data indicate that this white noise PM model is applicable over the range from about τ=1 day to about τ=1 to 2 weeks. This noise level allows one to measure at or beyond state-of-the-art limitations imposed by the standard.

B. Case B: Direct viewing of a single satellite for few minutes < τ < few hours.

The stability data shown in Figure 2 is a typical example using an NBS/GPS receiver with an omni-antenna. In this case the level of the white noise PM is such that MOD $\sigma_y(\tau=15\text{s})$=

5.8×10^{-10} with τ_h=15s. Coincidentally the RMS time fluctuations resulting from this configuration are also 5ns. Because τ_h is significantly different in case A and case B these noise levels are also quite different and arise from different mechanisms (a topic that could occupy another paper). One notices that for τ>1000s the fluctuations appear to be better modeled by the spectral density of the phase or time fluctuations going as f^{-3} (flicker noise frequency modulation, FM).

We conclude that averaging for longer than 1000s provides little or no improvement. The low frequency fluctuations generating the flicker noise FM spectra are probably caused by ionospheric and/or tropospheric delay fluctuations.

C. Case C: Viewing a single satellite for a few minutes each day for several successive days.

The data were taken from the USNO Series 4 publication for NAVSTAR 4, NAVSTAR 5, and NAVSTAR 6 (Space Vehicle 8, 5, & 9 respectively). One hundred and eighty four days of data were analyzed starting with 10 Nov. '81. As much as 23% of the days were missing from the published values. Interpolated values were filled in to avoid the problem of missing data in the analysis. Three obvious bad points were rejected over the first 100 days. The raw values with the interpolations are shown in Figure 3. There was obviously a rate change in the GPS clock at data point no. 109 of about 100 ns/day.

If one looks at the residuals, after fitting linear trends to the data some interesting results are seen. Using the last 74 days (since no bad data points had to be rejected from this set) we subtracted a linear least squares line from the UTC(USNO-MC) - GPS via NAVSTAR 4, 5, & 6. The mean slope removed by the linear least squares fit and the residuals are shown in Figure 4. Notice that the peak-to-peak deviation in the mean slopes removed was only about 4×10^{-15}. Also notice the high correlation in the long term (as it should be) since each satellite is being used to deduce the time difference between the same pair of clocks, UTC(USNO-MC) - GPS. That is, in long-term the relative clock noise predominates. In the day to day fluctuations, however, these uncorrelated processes probably arise from measurements made at varying times of day, through different parts of the ionosphere, and/or errors in satellites' ephemeris and up-load values. We can use the "three corner hat" routine to deduce the individual variances for each of the three satellites and their links. Figure 5 is such a stability diagram. The noise level is higher and not as well modeled as the common-view case, but still for sample times of a few days the white noise PM model seems to be reasonable, but breaks down for τ of the order of 1×10^6s and longer. The RMS time or phase fluctuations range from about 6ns to 11ns for these data. Figure 6 shows the UTC(USNO-MC) vs. GPS via NAVSTAR 5. Taking the difference between these variances will give the sum of the variances for the UTC(USNO-MC) and the GPS clock plus the variance for the correlated portion of the noise, which is then an upper limit on the clock's noise. Since we have reasonable confidence of the estimates for 1, 2, & 4 days we have calculated MOD $\sigma_y(\tau)$ for these sample times:

12.2×10^{-14}, 7.0×10^{-14}, 4.0×10^{-14}

respectively. This technique gives a nice way to compare the stabilities of two remote standards at the parts in 10 to the 14th level.

SIMULATION AND KALMAN FILTERS FOR GPS

A. Simulations

Over the past 15 years, scientists have developed reliable stochastic models of clocks and oscillators. Of course, these models cannot replace actual data, however, they can be used to predict performance of complex systems in advance of construction. Further, so much reliance on these models has developed, that if a model should actually fail, then the opportunity to refine the models would be quite significant.

The complexity of many systems poses problems for analytic solutions for system performance. Often one can become so greatly enmeshed in the mathematics of analytic solutions that the real problems become lost in a forest of equations. Of course, even the analytic solutions depend on model assumptions as much as the simulations. The advantage of analytic solutions is that often their extension to new parameter values is very simple and an "exact" solution is provided. In contrast, simulations using Monte Carlo trials can use much computer time and provide only an approximate value. Clearly, both simulations and analytic solutions have their advantages.

There is another potential problem with computer simulations and Monte Carlo trials. By virtue of the random character of the data, one could use strong selection criteria and influence the findings by presenting non-representive results. In this paper, seed numbers were chosen initially, and used throughout all simulations. As a further safe-guard, the simulation algorithm is included in the Appendix. Thus a critical reader can verify the results, and test the "representativeness" of the conclusions.

B. Stochastic Model

For times longer than a few seconds, commercial cesium beam clocks typically display frequency fluctuations which can be modeled well with three elements:

1) White noise FM.
2) Random walk noise FM, and
3) Linear frequency drift.

It should be mentioned that the linear frequency drift model tends to be more difficult in practice. Although one could add various failure modes to this model, they will be ignored here. Further, the present paper is concerned with sufficiently short durations that the third element, drift, will also be ignored. Thus, we are left with a two-element model for the clock: white FM, and random walk FM.
Mathematically, this can be represented as the sum of two processes:

$\Delta x'_n = \varepsilon_n$ and

$\Delta^2 x''_n = \eta_{n-1}$

where ε_n and η_n are random, independent variables with zero mean, normal distributions, and variances of σ_ε^2 and σ_η^2 respectively; and Δ and Δ^2 are the first and second difference operators, respectively. The clock model is totally represented by the sum of these processes given by

$$X_n = X'_n + X''_n, \text{ or}$$

$$\Delta^2 X_n = \eta_{n-1} + \Delta\varepsilon_n \qquad (1)$$

The parameters, σ_ε and σ_η along with the time interval between data samples, τ_o, are taken to have the following values:

Clock type	σ_ε	σ_η	τ_o
Conventional cesium beam	10 ns	3 ns	1 day
Option 004	3 ns	1 ns	1 day

(Note, the numerical values of σ_ε and σ_η are dependent on the sample interval, τ_o.

The Allan variance can be expressed as a function of these parameters with the following equation:

$$\sigma_y^2\,(N\tau_o) = \frac{\sigma_\varepsilon^2}{N\tau_o^2} + \frac{\sigma_\eta^2(2N^2+1)}{6N\tau_o^2} \qquad (2)$$

where N may take on any value.
Figure 7 is a plot of the square root of the Allan Variance deduced from Eq. 2 and the parameters given in the above table. This model for the slave clock (relative to whatever master clock is being referenced), can be expressed in the familiar terms of Kalman Filters (6).

$$\begin{bmatrix} X \\ Y \end{bmatrix}_n = \begin{bmatrix} 1 & 1 \\ 0 & 1 \end{bmatrix} \begin{bmatrix} X \\ Y \end{bmatrix}_{n-1} + \begin{bmatrix} \varepsilon \\ \eta \end{bmatrix}_n$$

$$\underline{H} = [1 \quad 0]$$

$$\underline{Q} = \begin{bmatrix} \sigma_\varepsilon^2 & 0 \\ 0 & \sigma_\eta^2 \end{bmatrix}$$

A little algebra can quickly show that this Kalman model is exactly equivalent to the clock model presented in Eq. (1). In addition to the clock model, the noise of the comparison link must be modeled also. The link noise appears to be random, uncorrelated (i.e., white) as has been found in the measurements reported above. Future experiments with different baselines and additional data may well refine this model of the comparison link, but for now the white phase model is in accord with observations. Thus the Kalman model is completed by introducing the variance of the measurement noise, R, according to the table below:

Comparison Mode	Value R	range	τ_h
Common View (4 satellites)	5 ns	≥1 day	600 s
One Satellite (short term)	5 ns	15 s to 900s	15 s
One Satellite ($\tau \geq 1$ day)	6-20 ns	≥1 day	600 s

where τ_h is the reciprocal software bandwidth (5).

The computer program used in the simulations can be found in the Appendix.

RESULTS AND COMPARISONS

In section II we characterized the noise performance of the GPS link for the three cases under consideration. Along with the models developed from these characterizations we use as typical clock models those shown in Figure 7 for a standard commercial cesium and for a high performance option 004 cesium. Which clock model one uses, of course, depends on the actual measurement configuration. We simulated the three cases being studied in this paper, but the theory developed is applicable to a much broader set of cases and clocks.

In case A we simulated the common-view link noise. The stability of the resulting simulated link noise processed by the Kalman filter is shown in Figure 8, which is better than state-of-the-art clocks for sample times of a few days and longer. Thus, for a few days and longer, the oscillator noise predominates. For comparison purposes the calculated stability from real data using a 10 day simple mean is indicated by the solid square. The excellent agreement is not suprising when one realizes that the optimum estimate of a constant buried in a white process is the simple mean. In practice what is done is to calculate the least square fit to the time differences over a 10 day period, and the slope then gives a nearly optimum estimate of the frequency difference between the clocks in the presence of white noise PM. The advantage of the Kalman output is that it gives in real time a daily optimum estimate of both the time and the frequency differences between the two remote clocks.

For the same level of link noise (5ns RMS), Figures 9 and 10 show the simulated time errors before and after the Kalman update as well as just after the Kalman update for a standard cesium and for an option 004 cesium respectively. Figure 11 graphically illustrates for a standard cesium the effects of looking at the clock just before update and just after update as indicated by the light and dark open squares respectively. The Kalman update stability values would, of course, be much closer together for the option 004 cesium.

For case B we simulated a standard cesium (comparable to those aboard the GPS satellites) and the 5ns link noise. The purpose was to test the improvement gained by the Kalman filter. Figures 12 and 13 are the results of that simulation. One sees about a 40dB improvement in stability for the Kalman output at τ=15s. In fact except for a small turn-on transient (not shown) the Kalman filter output tracks nearly perfectly the on board clock's time, and stability levels of a few in 10 to the 12 seem reasonably achievable.

For case C we use the Kalman filter to process the actual data. Figure 14 is a plot of the residual time differences between UTC(USNO-MC) - GPS via NAVSTAR 5 both with and without the Kalman filter. It is obvious that it acts like a low pass filter and one could design a simple recursive (exponential) filter to approach the Optimum. However, the number of lines of code are so few for the Kalman filter (as shown in the Appendix) that little would be gained. Figure 15 nicely illustrates this improvement in stability for sample times shorter than 10 days. At τ=1 day there is an 11 dB improvement in stability using the Kalman filter over the stability of the raw data.

From the data studied in this paper, there are clear advantages in proper filtering. Despite the fact that the data studied is not comprehensive and that the GPS receivers used were a limited set, one can still draw some reasonable and impressive conclusions. Table 1 is a summary of the stability and accuracy ranges of F&T calibrations available using GPS for remote clocks within about 3000 km of a primary reference.

CONCLUSIONS AND FUTURE WORK

The advent of GPS has produced a significant step forward in the accuracies and stabilities with which time and frequency can be compared at remote sites. With appropriate filtering of GPS data as outlined in this paper one can compare and calibrate remote clocks at state-of-the-art accuracies for sample times of the order of a few days and longer; e.g., a few parts in 10 to the 15 are achievable for averaging times of 10 days, and time accuracies of better than 10ns have been verified. The cesium standards on board GPS satellites may be used as accurate frequency references at the part in 10 to the 12 level. Even for short-term measurements of about 10 minutes duration nearly the full accuracy of these on-board cesiums can be transferred using appropriate data filtering as outlined above.

Future work will involve studies of world wide baselines leading to better understanding of the propogation medium's effects on GPS T&F measurements. Because the common-view approach appears to work even better than initially calculated, we have started some special studies. Some of the data indicates that there may be significant amounts of common-mode cancelation of errors due to a breathing effect working simultaneously across the ionosphere. This should be studied further. Stearable high gain antennas would lead to better time stabilities and perhaps better accuracies as multipath problems are reduced significantly. More accurate time transfers will result as people take advantage of the two frequencies radiated from the GPS satellites --giving a real time calibration of the ionosphere. The results of these research efforts suggest that the GPS system can support world-wide time and frequency comparison accuracies approaching a nanosecond and 1 part in 10 to the 15 respectively. The key questions, of course are regarding the availability of reasonably priced commercial receivers and continued access to the GPS constellation at full accuracy.

Acknowledgements

We are deeply appreciative of the suppport of the research staff at NBS including Dick Davis, Marc Weiss, Al Clements, Jim Jespersen and Trudi Peppler. The cooperation of the USNO staff has also been excellent and is much appreciated. Without the support of Air Force Space Division, Jet Propulsion Laboratories, Navy Metrology Engineering Center and Naval Air Logistics Center this work would not have been possible, and we express to them also our deep appreciation.

References

1) D. Allan and M. Weiss, "Accurate Time and Frequency Transfer During Common-View of a GPS Satellite", Proc. 34th Annual Symposium on Frequency Control, 334 (1980).
2) D. Davis, M. Weiss, A. Clements, and D. Allan, "Construction and Performance Characteristics of a Prototype NBS/GPA Receiver", Annual Symosium on Frequency Control, 1981.
3) D. Davis, M. Weiss, A. Clements, and D. Allan, "Unprecedented Syntonization and Synchronization Accuracy Via Simultaneous Viewing with GPS Receivers: Construction Characteristics of an NBS/

GPS Receiver" 13th Annual PTTI, 1-3 Dec. 1981.
4) J. Barnes, (A. Chi, L. Culter, D. Healey, D. Leeson, T. McGunigal, J. Mullen, W. Smith R. Sydnor, R. Vessot, and G. Winkler), "Characterization of Frequency Stability", NBS Technical Note 394 (Oct. 1970).
5) Allan and Barnes, "A Modified Allan Variance" with Increased Oscillator Characterization Ability, Proc. 35th Annual Synposium on Frequency Control 1981.
6) Gelb, Arthur, "Applied Optimal Estimation" The M.I.T. Press; Copyright 1974 by the Analytic Science Corporation.

APPENDIX

Attached are two copies of a computer program (in "BASIC") designed to (1) simulate the performance of typical cesium beam clocks, (2) simulate the comparison noise, and (3) operate on the simulated measurements with a Kalman Filter to obtain an optimum estimate of the clock's time. The constants listed in the program are chosen to simulate an average commercial cesium clock. The units are in nanoseconds and the time interval is one day. Other values of the sampling interval require different numerical values for the sigmas.

The data used for the Kalman Filter corresponds to the data which might actually be available in a real situation. Within the program, however, the "true" time is known Thus it is possible to evaluate the absolute performance of the Filter operating on the simulated data. A slight modification of this program was used with real data as reported in the text.

The first copy of the program has numerous remarks (prefaced by "REM") to aid in the understanding of the program. These "REMarks" are ignored by the operating program. The second version of the program is identical to the first, except that all remarks have been deleted and the steps renumbered. The second version was included to demonstrate how simple the Kalman Filter (which is only a part of the program) can really be.

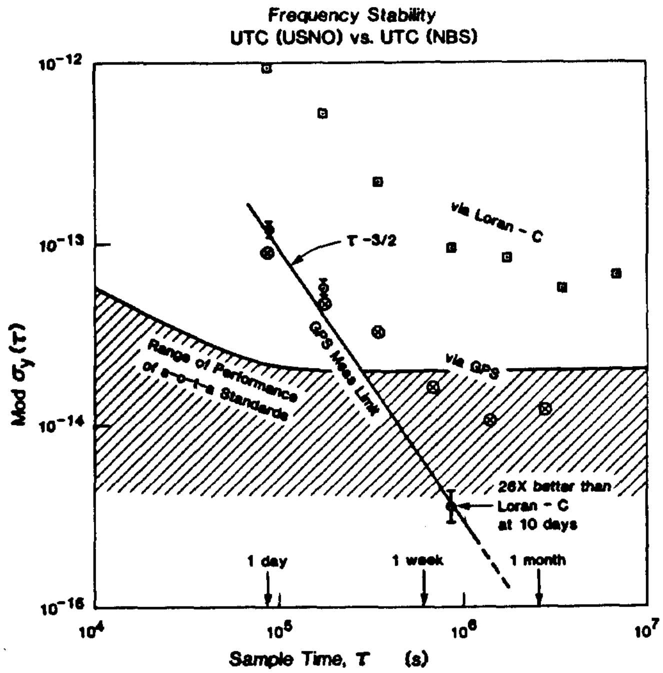

Figure 1

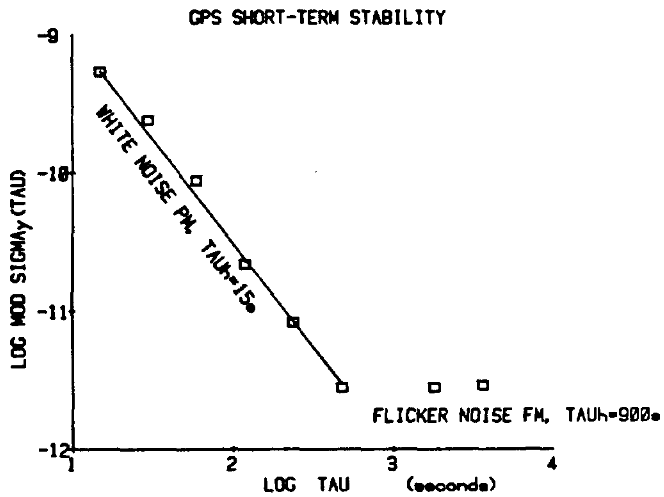

Figure 2

Table 1

For Kalman Filtered Data

CASE	Synchronization Accuracy	Time Stability	Syntonization Accuracy	Frequency Stability
A: Common-view	<10ns	~3.6ns τ_0=1 day	$<1\times10^{-14}$	$<3.5\times10^{-15}$ τ=10 days
B: Single Satellite Short-term	<50ns	~0.7ns τ_0=15s	$\sim2\times10^{-12}$	$\cong 2\times10^{-12}$ τ≅1000s
C: Single Satellite τ≥1 day	<20ns	~4.4ns τ_0=1 day	$\lesssim2\times10^{-14}$	$\cong1\times10^{-14}$ τ≅ 10 days

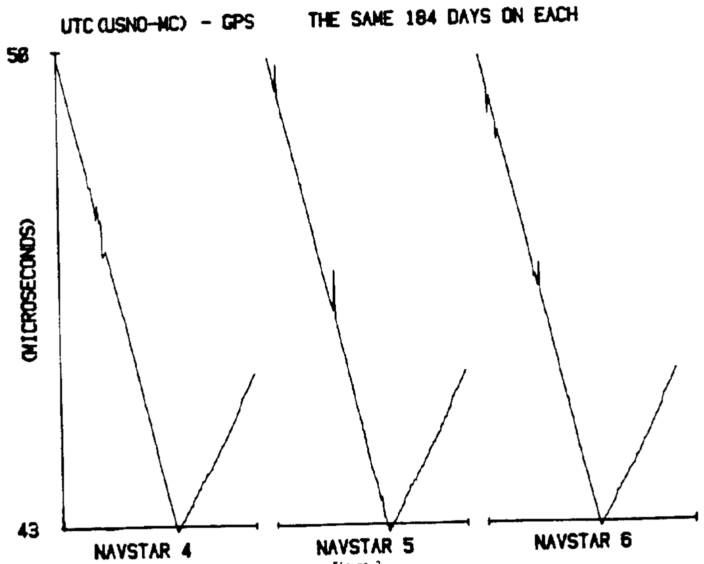

Figure 3

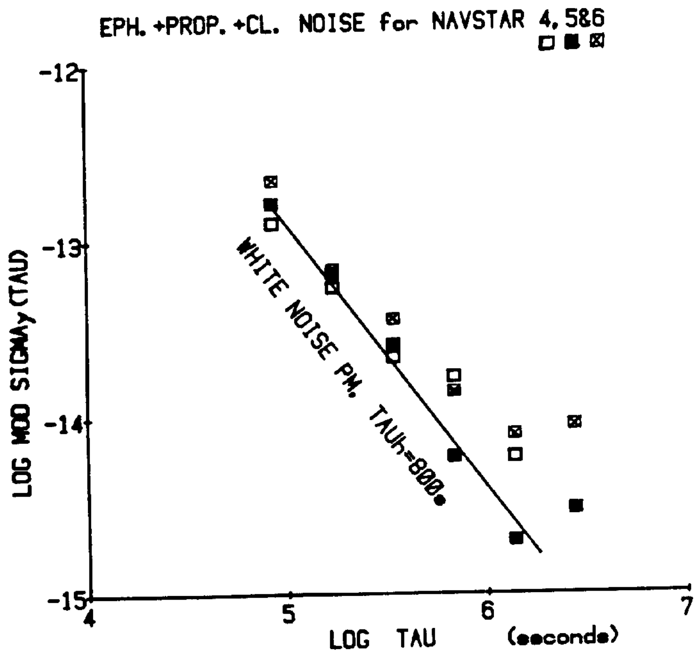

Figure 5

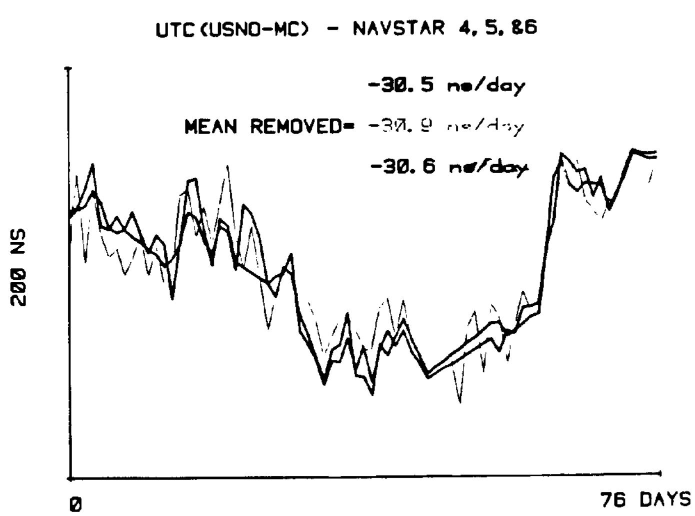

Figure 4

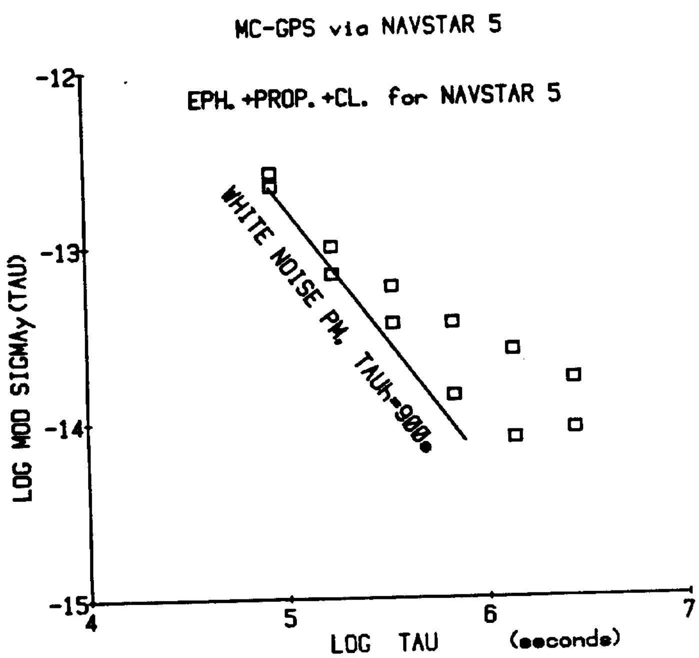

Figure 6

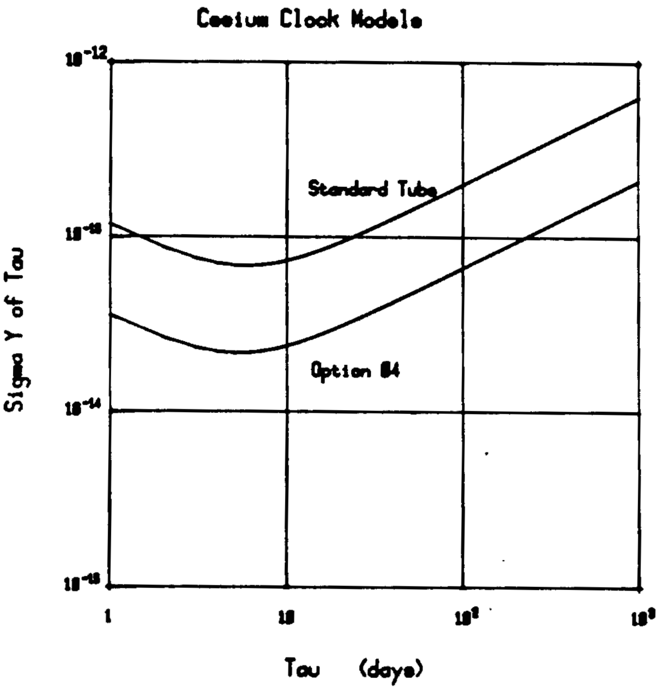

Figure 7

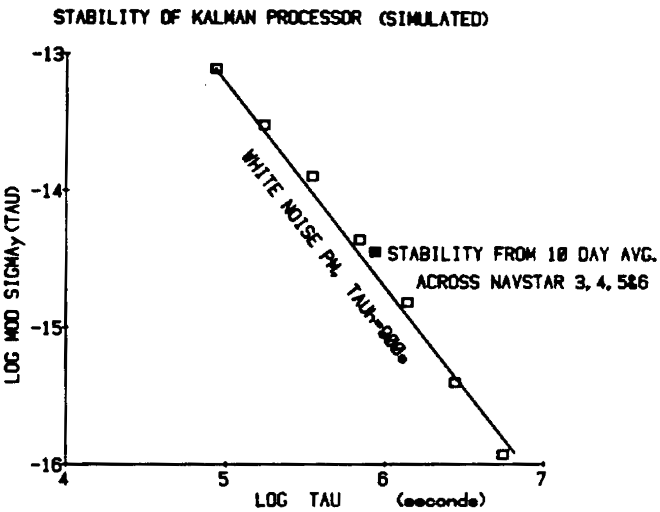

Figure 8

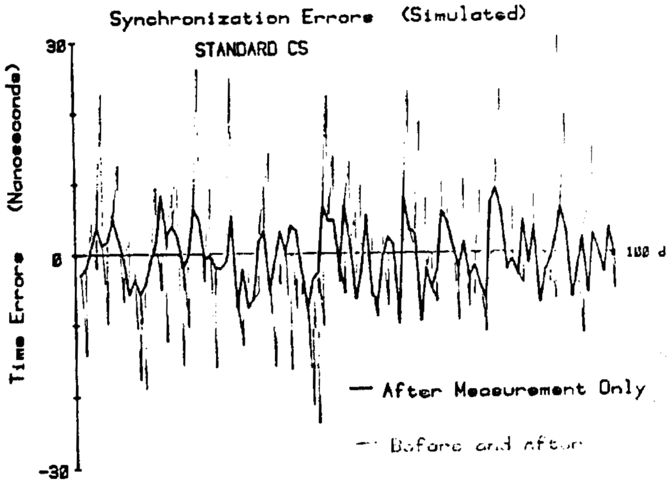

Figure 9

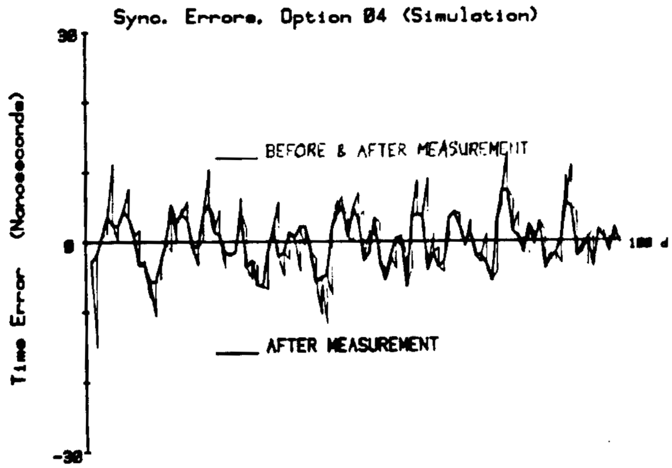

Figure 10

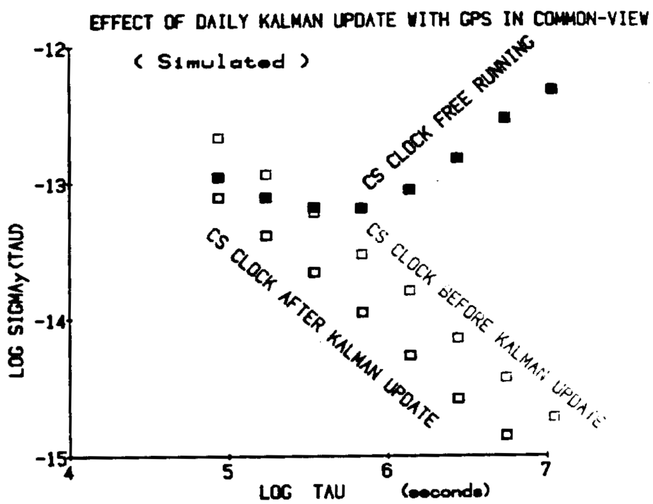

Figure 11

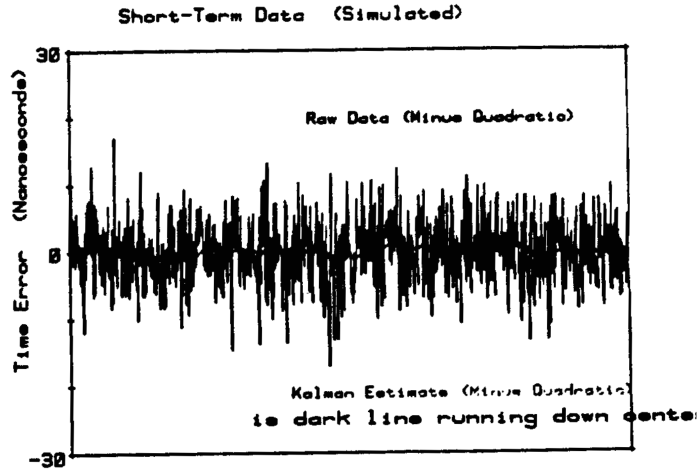

Figure 12

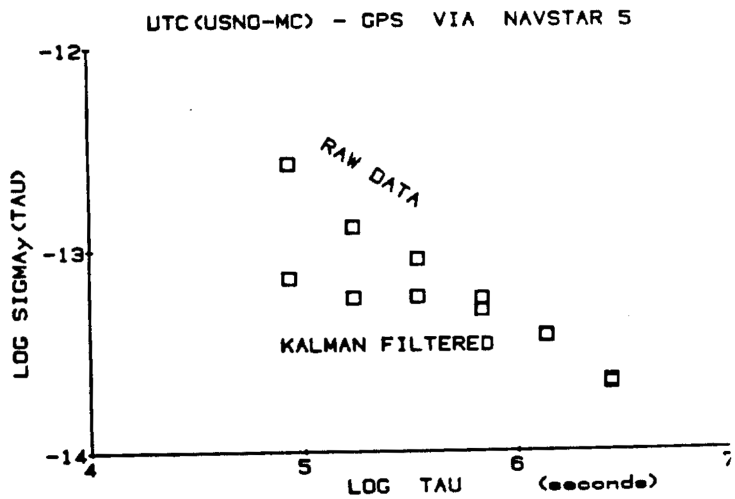

Figure 15

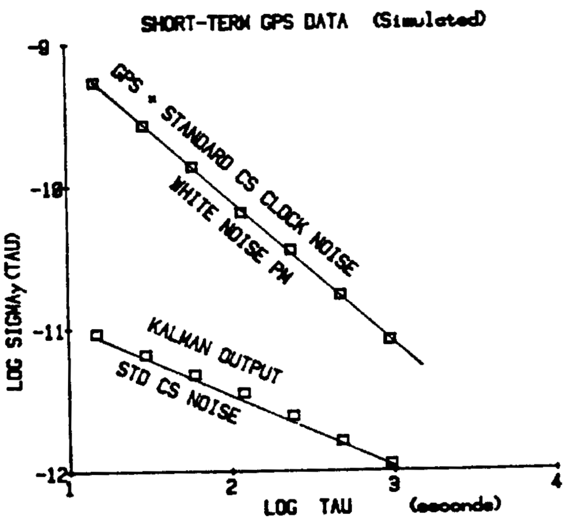

Figure 13

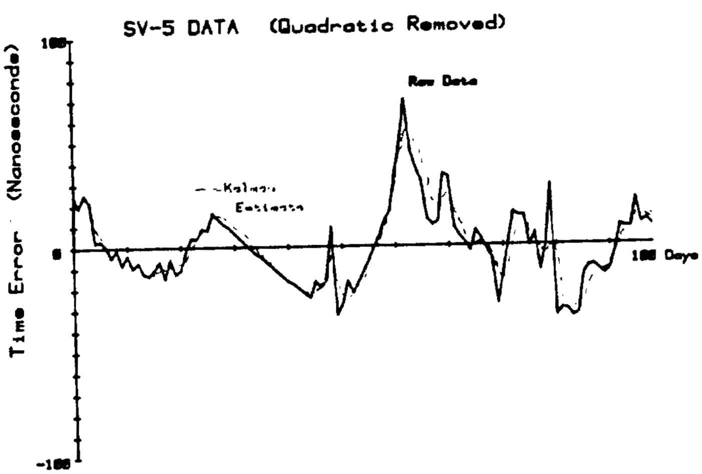

Figure 14

COMPUTER PROGRAM

```
LIST 1,499

100  REM  THIS PROGRAM SIMULATES
105  REM    THE GPS SATELLITES,
110  REM  PROPOGATION NOISE, AND
115  REM  THE SLAVE CLOCK.
120  REM  THE SLAVE CLOCK IS
125  REM   CORRECTED BY THE USE
130  REM   OF A KALMAN FILTER.
135  REM
140  REM
200  REM  SET CONSTANTS
202  REM   UNITS: NANOSEC &DAYS
205 P =  RND ( - 13.3371)
207  REM   SEED FOR RAND NO.
210 SE = 10: REM   WHITE FM
215 SN = 3: REM   RANDOM WALK FM
220 S = 5: REM   WHITE PHASE
223  REM  INITIAL CONDITIONS
225 X = 5000: REM  TIME ERROR
230 Y =  - 10: REM  FREQ BIAS
235 A = 2E7: REM  TIME VARIANCE
240 C = 1E4: REM  FREQ VARIANCE
250  REM
260  REM
300  FOR N = 1 TO 300
305  REM  SIMULATE 300 DAYS
310  REM
315  REM
400  REM  SIMULATE CESIUM BEAM
405  GOSUB 1000: REM   RANDOM NO.
       IN P
410 X = X + Y + SE * P: GOSUB 100
     0
415 Y = Y + SN * P: GOSUB 1000
420 Z = S * P: REM   LINK NOISE
430  REM
440  REM
450  REM  CALCULATE COVAR MATRIX-

451  REM
452  REM         ( A  B )
453  REM    P- = (      )
454  REM         ( B  C )
455  REM
456  REM
460 A = A + 2 * B + C + SE ^ 2
465 B = B + C:C = C + SN ^ 2
470  REM  FORECAST X1-, AND Y1-
475 X1 = X1 + Y1:Y1 = Y1
480  REM
485  REM
500  REM   COMPUTE MEASUREMENT
505 E = X + Z - X1: REM  CLOCK +
     LINK - FORECAST
507  REM
510  REM   THE QUANTITY X-X1
511  REM  IS THE FORECAST ERROR.
512  REM  IT IS ALSO THE ERROR
513  REM  JUST BEFORE CORRECTION
520  REM
530  REM
600  REM   UPDATE COVAR MATRIX+
605 U1 = A:U2 = B:R = A + S * S
615  REM  KALMAN GAIN K
620 K1 = U1 / R:K2 = U2 / R
625 A = A - U1 * K1
630 B = B - U1 * K2
635 C = C - U2 * K2
637  REM
638  REM
639  REM         ( A  B )
640  REM    P+ = (      )
641  REM         ( B  C )
642  REM
643  REM
650  REM   UPDATE X1+,Y1+
655 X1 = X1 + K1 * E
660 Y1 = Y1 + K2 * E
670  REM
680  REM
700  REM   THE TIME ERROR
702  REM  IS THE DIFFERENCE
704  REM  BETWEEN ACTUAL
705  REM  CLOCK, X, AND
707  REM  THE KALMAN ESTIMATE X1
710  PRINT N,X - X1
720  NEXT N
1000  REM  RANDOM NUMBER GEN
1005  REM  ZERO MEAN, UNIT VAR
1010 P = 0
1020  FOR J = 1 TO 6
1030 P = P +  RND (1) -  RND (1)
1040  NEXT J
1050  RETURN
```

SIMPLE PROGRAM

```
]LIST

100 P =  RND ( - 13.3371)
110 SE = 10
120 SN = 3
130 S = 5
140 X = 5000
150 Y =  - 10
160 A = 2E7
170 C = 1E4
180  FOR N = 1 TO 300
190  GOSUB 360
200 X = X + Y + SE * P: GOSUB 360

210 Y = Y + SN * P: GOSUB 360
220 Z = S * P
230 A = A + 2 * B + C + SE ^ 2
240 B = B + C:C = C + SN ^ 2
250 X1 = X1 + Y1:Y1 = Y1
260 E = X + Z - X1
270 U1 = A:U2 = B:R = A + S * S
280 K1 = U1 / R:K2 = U2 / R
290 A = A - U1 * K1
300 B = B - U1 * K2
310 C = C - U2 * K2
320 X1 = X1 + K1 * E
330 Y1 = Y1 + K2 * E
340  PRINT N,X - X1
350  NEXT N
360 P = 0
370  FOR J = 1 TO 6
380 P = P +  RND (1) -  RND (1)
390  NEXT J
400  RETURN
```